First Demonstration of Rotational Transform Control by Electron Cyclotron Current Drive in Large Helical Device

Takashi NOTAKE, Takashi SHIMOZUMA, Shin KUBO, Hiroshi IDEI[1], Katsumi IDA,
Kiyomasa WATANABE, Satoru SAKAKIBARA, Taiki YAMAGUCHI[2],
Mikirou YOSHINUMA, Takashi KOBUCHI[3], Shigeru INAGAKI[1], Tokihiko TOKUZAWA,
Yasuo YOSHIMURA, Hiroe IGAMI, Tetsuo SEKI, Hitoshi TANAKA[4],
Kazunobu NAGASAKI[4] and LHD Experimental Group

National Institute for Fusion Science, Toki, Gifu 509-5292, Japan
[1]*Research Institute for Applied Mechanics, Kyushu University, Fukuoka 816-8580, Japan*
[2]*Fusion Research Development Division, Japan Atomic Energy Agency, Naka 311-0193, Japan*
[3]*Faculty of engineering, Tohoku University, Sendai 980-8579, Japan*
[4]*Graduate school of Energy Science, Kyoto University, Kyoto 606-8501, Japan*

An active current drive is a promising technique for improving plasma performances by controlling rotational transform and/or magnetic shear profiles in helical devices. A current drive based on electron cyclotron resonance heating is the most appropriate scheme for this purpose in terms of locality of driven current. Optimum conditions for an efficient electron cyclotron current drive (ECCD) in Large Helical Device (LHD) are being investigated using three-dimensional ray-tracing code, which can simulate propagation and power dissipation of electron cyclotron waves with large parallel refractive index. In the present experiment, inversion of directions of driven plasma current corresponding to injected ECCD modes was demonstrated successfully, and the results could be elucidated by the Fisch-Boozer theory. In addition, clear shifts of rotational transform were observed by motional Stark effect polarimetry. Our findings verified that the ECCD can be used as an effective actuator for controlling the rotational transform and magnetic shear profile in LHD.

1. Introduction

Non-inductive current drives have been investigated in several tokamak devices [1–3], because they are vital for steady-state operation of tokamak-type fusion reactors. In contrast to tokamaks, heliotron devices do not require a non-inductive current drive for formation of magnetic field lines to confine plasma. However, finite plasma pressure gradients and injected strong neutral beams induce plasma currents spontaneously, resulting in the change of magnetic field structures such as rotational transform and magnetic shear, and then in degradation of fusion plasma performance. Therefore, the use of non-inductive current drives for controlling plasma currents and magnetic field structures is one of significant themes in helical devices.

Several schemes similar to the non-inductive current drive actuators are being studied. Notably, the electron cyclotron current drive (ECCD) appears to be a promising candidate for controlling a plasma current profile, because the power transitions from electron cyclotron waves to resonant electrons in plasmas are extremely localized. Thus,

the ECCD exhibits merits such as locality and high density of driven plasma currents [4,5]. With the ECCD, we can also select the location of driven plasma currents almost arbitrarily by adjusting parameters such as magnetic field strength, wave frequency, and parallel refractive index. ECCD experiments have already been conducted not only in tokamak devices but also in helical devices with the aim of controlling the rotational transform and magnetic shear profile [6–9]. For example, in Wendelstein 7-AS stellarator and TJ-2 heliac, the magnetic shear is designed to be very weak in order to avoid the appearance of low-order rational surfaces near the plasma core regions. In Large Helical Device (LHD), on the contrary, moderate magnetic shear exists in the plasma core region despite the existence of low-order rational surfaces. Therefore, it is very important to study the relationships among magnetohydrodynamics (MHD) instabilities, low-order rational surfaces, rotational transform, magnetic shear, and plasma performance in an LHD, because the parameters responsible for plasma confinement vary with each experimental device. The ECCD must be a very effective technique for these studies and should be optimized for effective control

author's e-mail: notake@fir.fukui-u.ac.jp

of plasma current.

   This paper is organized as follows. The electron cyclotron resonance heating (ECRH) and ECCD systems used in LHD are briefly introduced in the next section. Section 3 describes an in-depth inspection for effective ECCD under the complex magnetic configuration of LHD. Experimental results and discussions are presented in Section 4. Finally, our research is summarized in Section 5.

2. ECCD System in LHD

   LHD is a heliotron device with pole number $l = 2$ and toroidal mode number $m = 10$. Its major radius, averaged minor radius, aspect ratio, and averaged plasma volume are 3.9 m, 0.6 m, about 7, and 25 m^3, respectively [10]. It has two continuous-winding superconducting helical coils, six superconducting poloidal coils, and twenty normal conducting local island divertor coils. Various magnetic configurations can be achieved by adjusting these external coil currents. For example, the position of the magnetic axis can be changed by controlling dipole magnetic fields, and the ellipticity of the plasma cross-section can be changed by controlling quadrature magnetic fields. The magnetic axis is located 3.75 m from the torus center in the standard magnetic configuration of LHD. Shifting the magnetic axis into the major radius improves neoclassical transport but degrades MHD properties based on the linear theory because of the "magnetic hill" effect. On the other hand, shifting the magnetic axis outward causes reverse change in the neoclassical and MHD properties in a theoretical sense.

   In an inward shifted configuration, improvements of anomalous transport were observed experimentally [11]. According to the linear MHD theory, it is predicted that some MHD instabilities affect plasma confinement in such a configuration. Nonlinear effects have been suggested as one of the reasons for the good confinement achieved in the configuration. These effects may prevent MHD activities from growing further. However, in order to extend the operational parameters of the LHD, MHD activities should be suppressed, because they always cause severe degradation of plasma confinement. The ECCD may possibly improve MHD properties by local current control alone without degrading both neoclassical and anomalous transports, even in the inward shifted configuration.

   Two schemes have been conceived for improving plasma confinement capability using the ECCD. One is "ECCD to co-direction" (Co-ECCD), which increases the rotational transform and results in the exclusion of low-order rational surfaces at the plasma core region, where the magnetic shear is very weak. The other is "ECCD to counter-direction" (Ctr-ECCD), which can locally enhance negative magnetic shear. Therefore, driving plasma current along arbitrary directions is desirable as a current drive actuator.

   The ECRH and ECCD systems have been upgraded

gradually, which now consist of three 168-GHz and five 84-GHz gyrotrons with a total injection power of about 2 MW. For the ECCD, the beam should be injected at an oblique angle to the toroidal direction. The toroidally movable antenna is installed at the 1.5 L and 2O ports of LHD. This paper reports the findings of ECCD obtained by using the 2O port antenna, where one 84-GHz and one 168-GHz gyrotrons are connected [12]. The high-power millimeter wave radiated from the gyrotron is converted into a Gaussian beam by phase correcting mirrors in the matching optics unit [13]. The beam is then transmitted to the antenna installed inside the vacuum vessel by oversized corrugated waveguides in order to reduce power losses [14]. The injection angle of the beam is varied both toroidally and poloidally using the final steering mirror. The polarization state of the beam can also be varied using a set of polarizers, i.e., two mirrors with different grating depths ($\lambda/4$ and $\lambda/8$) [15].

3. Oblique Ray Tracing for an ECCD

   The mechanism of deposition of an ECCD in an LHD is more complicated than that in tokamak devices because of the asymmetric three-dimensional magnetic field structure. Therefore, the optimum conditions for the ECCD need to be investigated by a ray-tracing calculation while considering the field structure.

   The ECCD mechanism is based on asymmetric distortion of electron resistivity in momentum space formed by selective energy interactions. The electron cyclotron waves are absorbed by electrons whose velocity component satisfies the following condition after taking Doppler up-shift and full relativistic down-shift into consideration [16, 17].

$$\frac{\omega^2 N_\parallel^2 + l^2 \Omega^2}{\omega^2 N_\parallel^2 + l^2 \Omega^2 - \omega^2} \left(\frac{v_\perp}{c}\right)^2$$
$$+ \frac{\omega^4 N_\parallel^4 + 2\omega^2 N_\parallel^2 l^2 \Omega^2 + l^4 \Omega^4}{\omega^2 N_\parallel^2 l^2 \Omega^2 + l^4 \Omega^4 - \omega^2 l^2 \Omega^2} \left(\frac{v_\parallel}{c} - \frac{\omega^2 N_\parallel}{\omega^2 N_\parallel^2 + l^2 \Omega^2}\right)^2 = 1$$

(1)

where $N_\parallel$, l, Ω, ω, $v_\perp$, $v_\parallel$, and c are the parallel refractive index, harmonic number of cyclotron resonance, cyclotron frequency, wave frequency, perpendicular thermal velocity, parallel thermal velocity, and light velocity, respectively.

   Fig. 1 gives an example of resonant curves in the momentum space under certain calculation parameters. The curves are represented as solid lines with numeric values that indicate strength of resonant magnetic fields at each position in the momentum space, and the circles drawn by dotted lines are contour plots of the velocity. In the case of large $N_\parallel$ injection, the resonant curves move to a high parallel velocity region in the velocity space because of strong up-shift of cyclotron resonance. A resonance occurs even in magnetic fields below 3 T, which corresponds to the fundamental resonance condition of ECRH for 84-GHz waves. These findings indicate that electron cyclotron
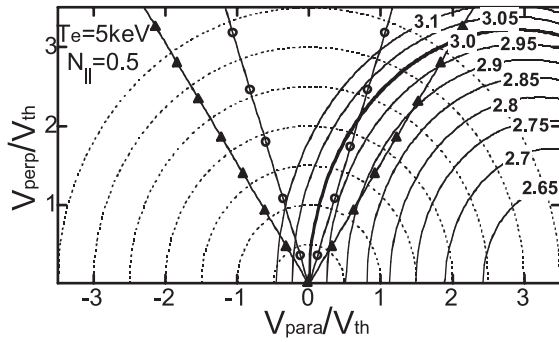
Fig. 1   Resonance curves in velocity space. Electron temperature, parallel refractive index, harmonic order number, and wave frequency are set to 5 keV, 0.5, 1, and 84 GHz, respectively.
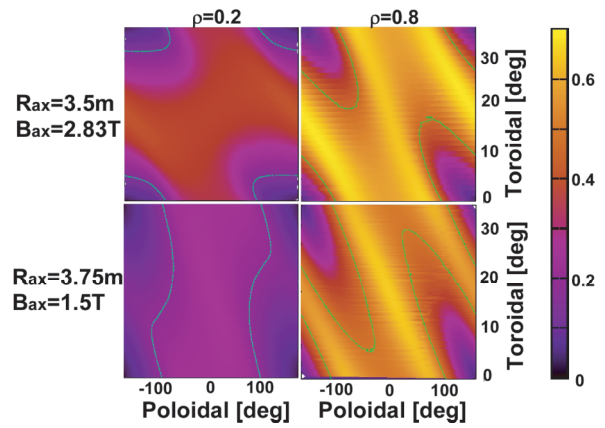

Fig. 2   Distributions of magnetic field strength normalized by maximum value on each flux surface. Zeros of toroidal and poloidal angles correspond to vertically elongated cross-section and inside of equatorial plane, respectively.

waves tend to interact with electrons having higher parallel velocity components. Therefore, electron cyclotron waves with large $N_{\parallel}$ must be effective in terms of collisionality in achieving high ECCD efficiency.

The electron trapping effect is another critical issue. Trapped electrons reduce the ECCD efficiency or may reverse the direction of the driven current because of the Ohkawa effect, as the diffusion in velocity space caused by electron cyclotron damping is mainly along the perpendicular direction. The two lines joining the open circles and closed triangles in Fig. 1 indicate the region within which an electron may be trapped by magnetic ripple. The line joining the open circles represents a weaker magnetic ripple. In particular, LHD has not only toroidicity but also helicity, and the ratio between the two depends strongly on the magnetic configuration. In order to avoid such difficulties, the wave power should ideally be deposited at the top of the magnetic ripple region. Fig. 2 shows the contour plots of magnetic ripples for the two magnetic configurations in LHD. The upper column corresponds to a magnetic axis of 3.5 m, which is one of the inward shifted configurations with low effective helicity. This configuration has good confinement performance owing to the improvement in neoclassical and anomalous transports; therefore, it is suitable for effective ECRH. On the other hand, the lower column shows magnetic ripples when the magnetic axis is set to 3.75 m, which is the standard magnetic configuration of LHD. This configuration may be more suitable from the viewpoint of ECCD efficiency, because it has hardly any magnetic ripple near the magnetic axis, and an improvement in the degradation of efficiency due to trapped electrons can be expected. In this configuration, however, only the X-mode ECCD at the second harmonic resonance using the 84-GHz gyrotron is available because of the limit on achievable magnetic field strength of 1.5 T. As shown in Fig. 2, the magnetic ripple is more enhanced in the peripheral regions; therefore, it is not possible to realize wave injection with large $N_{\parallel}$ mponent and deposit it at the weak magnetic ripple region because of the strong Doppler up-

shift of resonance. To study this phenomenon in greater detail, we need to solve the Fokker–Planck equation strictly in complex LHD configuration, because the trapping effects of current-carrying electrons in the magnetic ripple are decided by the subtle balance between diffusion and Coulomb collisional relaxation processes in momentum space. To conduct ECCD experiments at higher powers, we consider the optimum condition under the inward shifted configuration in this paper.

In order to investigate the optimum incident angles for the ECCD, we performed a ray-tracing calculation. Ray tracing is a sophisticated technique offering predictions on propagation and absorption of electron cyclotron waves in dispersant fusion plasmas. A ray-tracing code had been developed for ECRH under the three-dimensional magnetic field structure of LHD. However, the application of this code is limited to quasi-perpendicular waves propagating with respect to magnetic field lines in weakly relativistic thermal plasma [18]. Therefore, the existing ray-tracing code was modified in order to deal with obliquely propagating electron cyclotron waves. For propagation angles satisfying the following conditions [19]

$$N|\cos\theta| \gg |1 - l\Omega/\omega|, \tag{2}$$

and

$$N|\cos\theta| \gg v_{t}/c, \tag{3}$$

the relativistic down shift of the cyclotron frequency can be neglected, because the Doppler effect becomes more dominant. Here, θ and v_{t} represent propagation angle with respect to magnetic field lines and electron thermal velocity, respectively. We can therefore use absorption coefficients obtained from the non-relativistic dielectric tensor for a hot Maxwellian plasma. Under this treatment, the power absorption line is decided not from the Fq function but from
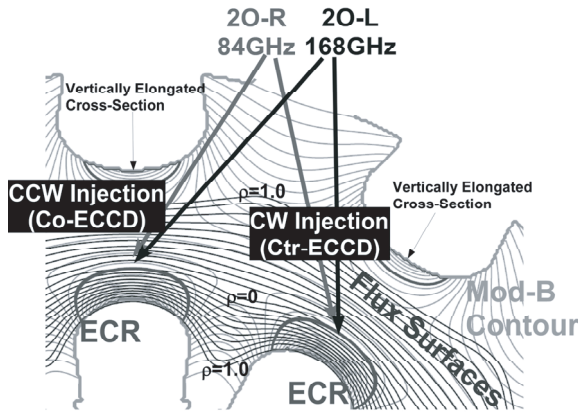
Fig. 3   ECCD configuration obtained using 2O-port antenna at the magnetic configuration of $R_{ax} = 3.5$ m. One 84-GHz and one 168-GHz gyrotrons are connected to 2O-port.
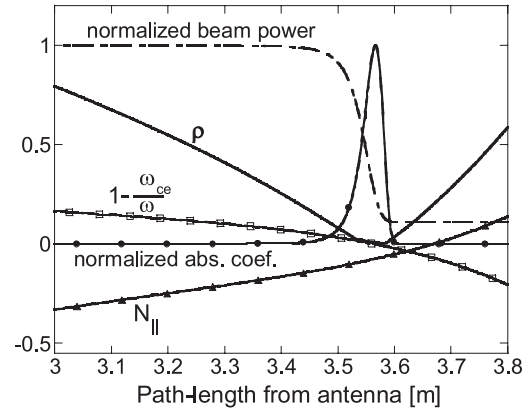

Fig. 4   Parameter changes along the central-ray injected from the 2O-port. Power absorption region is a little broader than normal ECRH due to the finite $N_\parallel$ effect.

the conventional Fried-Conte function expressed as

$$Z(\zeta) = i\sqrt{2}\exp(-\zeta^2)\int_{-\infty}^{\sqrt{2}i\zeta}\exp(-t^2/2)dt, \qquad (4)$$

which can be calculated numerically. Here, the argument ζ is defined as follows.

$$\zeta \equiv c(1 - \omega_c/\omega)/(\sqrt{2}v_t N\cos\theta). \qquad (5)$$

The 2O-port antennas installed at the horizontally elongated cross-section of LHD is suitable for the ECCD, because it can swing the beam along the toroidal direction over a wide range of angles. One 84-GHz and one 168-GHz gyrotron are connected to this port. Antennas radiating the 84- and 168-GHz beams are called 2O-R and 2O-L, respectively. These antennas are used to aim injection beams at the magnetic axis of neighboring vertically elongated cross-sections as shown in Fig. 3. According to the Fisch-Boozer theory [20], electrons circling the torus in the same direction as propagating electron cyclotron waves are accelerated to higher $v_\perp$ region in momentum space, and hence, lead to less collisions. As a result, plasma currents generated using the ECCD are supposed to flow in the clockwise (CW) and counterclockwise (CCW) directions if the beams are injected in the CCW and CW directions, respectively.

The ray-tracing calculations were performed with multiple rays (10 radial and 31 azimuthal) to imitate real Gaussian beams with a finite beam width. Typical electron temperature and density profiles obtained in experiments, which will be shown in the next section, were adopted in the calculations. Fig. 4 shows some parameter variations along the central ray. Here, the 3.5 m magnetic axis and an average magnetic field strength of 2.829 T were employed, and the 84-GHz beam with fundamental ordinary mode (O-mode) was aimed at the magnetic axis of the vertically elongated cross-section from the 2O-R antenna. This configuration allows on-axis ECCD, because

the power of electron cyclotron waves is absorbed almost completely within the normalized radius $\rho = 0.2$ in the plasma.

4. Experimental Results and Discussion

ECCD experiments were conducted in LHD using the 2O port antenna at a magnetic configuration of $R_{ax} = 3.5$ m. Magnetic field strength and injection angles were optimized based on the oblique ray-tracing code, as mentioned above. The ellipticity of incident wave polarization is a critical factor affecting the excitation of suitable modes in plasmas for effective ECCD. As shown in Fig. 5, a linearly polarized wave is required for normal perpendicular injection. However, some finite ellipticity, depending on the injection angles, is necessary for oblique injection, and the direction of rotation of the electric fields is opposite for the O- and extraordinary (X)- modes [21]. In the experiment, polarization is controlled using grating polarizers.

Fig. 6 shows the typical electron temperature and density profiles of target plasmas in the experiment. The temperature and density were measured using an electron cyclotron emission diagnostic and a far-infrared radiation interferometer, respectively. The electron internal transport barrier was formed by strongly focused ECRH, and the center electron temperature reached about 5 keV [22]. High electron temperature is desirable for realizing high absorption ratio by a single path. In addition, the electron density profile is a little hollow, as is typically observed in LHD. To achieve high ECCD efficiency, electron density is suppressed by controlling the gas puffing. As shown in Fig. 7, the target plasmas were produced and sustained by ECRH alone, in order to avoid the contribution of driven current generated by strong neutral beam injection (NBI). The additional ECRH and ECCD were superposed from 0.25 s for a duration of 0.5 s. A longer pulse duration is
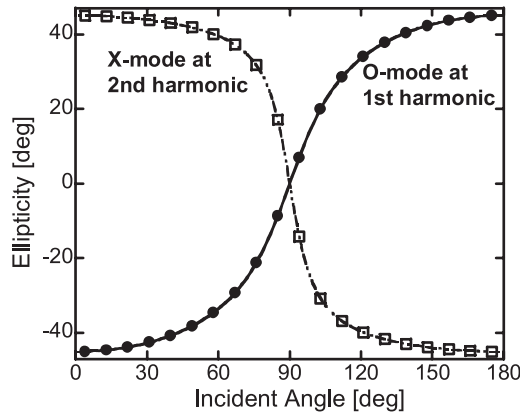
Fig. 5 Optimum incident ellipticities as a function of incident angles, which are defined as the angles between magnetic field lines and wavenumber vectors at the last closed flux surfaces.
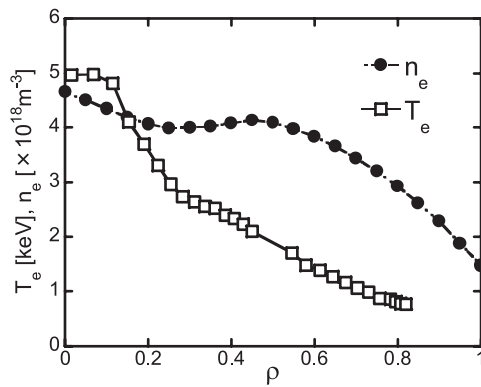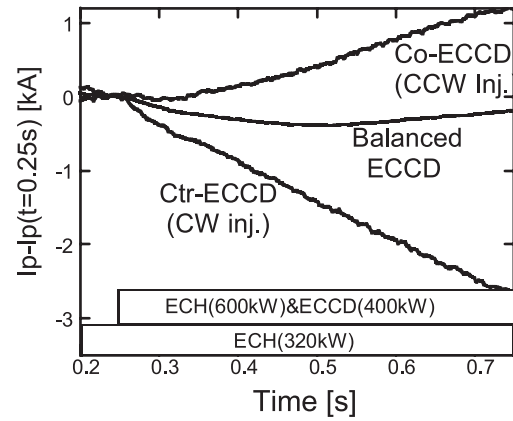

Fig. 7 Injected ECRH and ECCD timings and temporal evolutions of total plasma currents. Plasma currents are normalized by the values obtained at ECCD injection ($t = 0.25$ s).
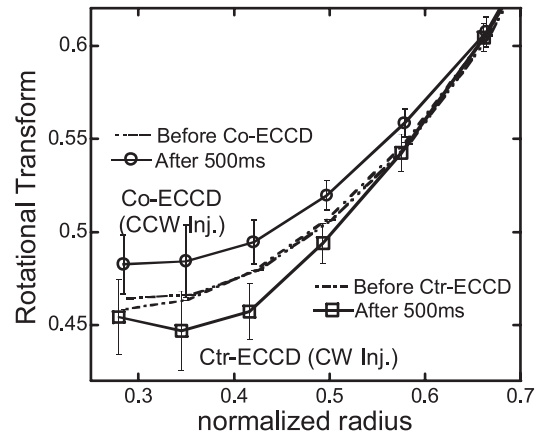

Fig. 6 Typical electron temperature and electron density profiles in the experiment. Electron internal transport barrier with steep gradients near the center is realized. Density profile is a little hollow.

Fig. 8 Radial profile of the shifts of rotational transform due to Co- and Ctr-ECCD diagnosed by the MSE measurement.

ideal; however, it was not attempted because of a slump in the gyrotron. The comparison of temporal evolutions of total plasma currents measured with a Rogowski coil is also shown in Fig. 7. Some differences in target plasma currents due to differences in the initial discharge conditions were observed. Therefore, the data were normalized by values obtained at 0.25 s in order to clarify the contribution of the ECCD to plasma currents.

The bootstrap current is a part of the total plasma current; however, its contribution is low, judging from the current data of the balanced ECCD discharge. In the experiment, a balanced ECCD was realized by injecting two beams from the 2O-port in opposite directions. For Co- and Ctr-ECCD discharges, the directions of the driven plasma current were clearly inverted and were consistent with those predicted by the Fisch-Boozer theory. Plasma current control using the ECCD was thus demonstrated successfully in LHD for the first time. However, the absolute values of plasma currents were still low because of

high electron temperature, resulting in a long resistive diffusion time of a few seconds compared with the ECCD duration. The current driven using the ECCD may therefore be cancelled to some extent by the induced back electromotive force. Such a canceling current may flow in the plasma peripheral region to cancel the magnetic flux produced using the ECCD. However, this affects the rotational transform shifts only weakly, as the current density was very small in the plasma peripheral region because of the large area of the flux surface.

Certain rotational transform shifts caused by the ECCD were also observed by motional Stark effect (MSE) polarimetry [23–25]; the results are given in Fig. 8. Here, it should be noted that this measurement was performed at a different magnetic configuration of $R_{ax} = 3.75$ m, because MSE polarimetry can only be applied to the peripheral regions of the $R_{ax} = 3.5$ m configuration. In addition to the ECCD, two neutral beams were also injected into these discharges as a probe beam for MSE measurement.

However, the contribution of NBI to plasma current was carefully suppressed by the balanced injection of the two beams at the same power. Fig. 8 represents the changes in the rotational transform as a result of the ECCD alone. The dot-dash lines indicate the rotational transform profiles before ECCD injection, i.e., the rotational transform profile in typical ECRH plasma. Solid lines joining the open circles and squares are the rotational transform profiles after 0.5 s of the Co- and Ctr-ECCD injections, respectively. The profiles show marked changes corresponding to the different ECCD modes, although the variations are not significantly large. These results, however, are encouraging from the viewpoint of controlling the magnetic field structure and thus improving the confinement capability of LHD plasma. Further experiments at higher powers and longer pulse durations are required to determine the effect on plasma performance due to modification of the plasma current profile and/or magnetic field structures.

5. Summary

The applicability of the ECCD was evaluated both theoretically and experimentally with the aim of controlling plasma current and magnetic field structures such as rotational transform and magnetic shear profiles in LHD. A ray-tracing code was developed for scrutiny of the ECCD. Experimental conditions such as the magnetic field configuration and incident wave parameters were optimized using the code. In the experiment, the inversion of the directions of driven plasma currents corresponding to the injected ECCD modes was observed clearly, thus indicating successful demonstration of plasma current control using the ECCD for the first time in LHD, because this inversion is consistent with theoretical predictions. In addition, significant changes in rotational transform profiles were verified by MSE polarimetery. Thus, the ECCD can be expected to play a key role in controlling the rotational transform profile and magnetic shear in LHD.

Acknowledgments

[1] O. Sauter, M.A. Henderson, F. Hofmann, T. Goodman *et al.*, Phys. Rev. Lett. **84**, 3322 (2000).
[2] T.C. Luce, Y.R. Lin-Liu, R.W. Harvey, G. Giruzzi *et al.*, Phys. Rev. Lett. **83**, 4550 (1999).
[3] T. Suzuki, S. Ide, K. Hamamatsu, A. Isayama, T. Fujita *et al.*, Nucl. Fusion **44**, 699 (2004).
[4] V. Erckmann and U. Gasparino, Plasma Phys. Control. Fusion **36**, 1869 (1994).
[5] R. Prater, Phys. Plasmas **11**, 2349 (2004).
[6] H. Maabberg, M. Rome, V. Erckmann *et al.*, Plasma Phys Control. Fusion **47**,1137 (2005).
[7] A. Fernandez *et al.*, to be published in Fusion Science and Technology.
[8] M. Rome, V. Erckmann, H.P. Laqua *et al.*, Plasma Phys. Control. Fusion **45**, 783 (2003).
[9] V. Tribaldos, J.A. Jimenez, J. Guasp and B.P. Milligen, Plasma Phys. Control. Fusion **40**, 2113 (1998).
[10] O. Motojima, H. Yamada, A. Komori, N. Ohyabu *et al.*, Nucl. Fusion **47**, 668 (2007).
[11] A. Komori, N. Ohyabu, H. Yamada, O. Kaneko *et al.*, Plasma Phys. Control. Fusion **45**, 671 (2003).
[12] T. Notake, S. Ito, S. Kubo *et al.*, Trans. Fusion Scie. Technol. **51**, 409 (2007).
[13] T. Notake, H. Idei, T. Shimozuma, M. Sato *et al.*, Fusion Eng. Des. **73**, 9 (2005).
[14] J.L. Doane, *Infrared and Millimeter Waves* **13**, chapter 5 (1985).
[15] T. Notake, H. Idei, S. Kubo, T.Shimozuma *et al.*, Rev. Sci. Instrum. **76**, 023504 (2005).
[16] P.U. Lamalle *et al.*, Trans. Fusion Sci. Technol. **45**, 153 (2004).
[17] E. Westerhof *et al.*, Trans. Fusion Sci. Technol. **45**, 159 (2004).
[18] S. Kubo, T. Shimozuma, H. Idei *et al.*, J. Plasma Fusion Res. Series **5**, 584 (2002).
[19] M.Bornatciti, Nucl. Fusion **23**, 1153 (1983).
[20] Nathaniel J. Fisch, Rev. Mod. Phys. **59**, 175 (1987).
[21] T. Notake, S. Kubo, T.Shimozuma *et al.*, Plasma Phys. Control. Fusion **47**, 531 (2005).
[22] T. Shimozuma, S. Kubo, H. Idei, S. Inagaki *et al.*, Nucl. Fusion **45**, 1396 (2005).
[23] F.M. Levinton, R.J. Fonck *et al.*, Phys. Rev. lett. **63**, 2060 (1989).
[24] T. Suzuki, S. Ide, T. Oikawa *et al.*, Plasma Phys. and Control. Fusion **44**, 1 (2002).
[25] K. Ida, M. Yoshinuma, K.Y. Watanabe *et al.*, Rev. Sci. Instrum. **76**, 053505 (2005).